$^{19}F(p, \alpha)^{16}O$ and $^{19}F(\alpha,p)^{22}Ne$ Reaction Rate Measured via THM and Fluorine Nucleosynthesis in AGB stars

IOP Conf. Series: Journal of Physics: Conf. Series **1308** (2019) 012016 doi:10.1088/1742-6596/1308/1/012016

^{19}F(p,α)^{16}O and ^{19}F(α,p)^{22}Ne Reaction Rate Measured via THM and Fluorine Nucleosynthesis in AGB stars

S. Palmerini[1,2], G. D'Agata[3], M. La Cognata[4], I. Indelicato[4], R. G. Pizzone[4], O. Trippella[2] and D. Vescovi[2,5]

[1] Dipartimento di Fisica e Geologia, Università degli Studi di Perugia, via A. Pascoli, I-06125 Perugia, Italy
[2] I.N.F.N. sezione di Perugia, via A. Pascoli, I-06125 Perugia, Italy
[3] Nuclear Physics Institute of the Czech Academy of Sciences, p.r.i., Řež 130, Řež, 25068 Czech Republic
[4] I.N.F.N. Laboratori Nazionali del Sud, Via Santa Sofia 62, I-95123, Catania, Italy
[5] Gran Sasso Science Institute, Viale Francesco Crispi, 7, 67100 L'Aquila, Italy

E-mail: sara.palmerini@pg.infn.it

Abstract. Asymptotic Giant Branch (AGB) stars have been proven to be sites of F production through spectroscopy observations by several authors, but it is not clear whether these stars might account for the total fluorine abundance of the Galaxy. Recently the two main channels for ^{19}F destruction in AGB stars, namely the ^{19}F(α,p)^{22}Ne and ^{19}F(p,α)^{16}O reactions, have been studied via the Trojan Horse Method in the energy range of interest for astrophysics. In both cases experimental results have shown the presence of resonant structures below 500 keV, hinting to an enhancements in efficiency of fluorine destruction by stellar H- and He- burning. In particular the ^{19}F(p,α)^{16}O reaction rate at $T_9 \leq 0.2K$ turns out to be increased up to a factor of 1.7 while the ^{19}F(p,α)^{16}O is enhanced more than a factor of 4 at $0.1 \leq T_9 \leq 0.25$. We present here a re-analysis of the role of AGB stars as fluorine galactic source by comparing stellar observations with predictions of AGB nucleosynthesis (for stellar masses from 1.5 to 5M$_\odot$) computed by employing in state-of-the-art models the THM reaction rates for ^{19}F destruction.

1. Introduction

The sole stable isotope of fluorine, the ^{19}F, is produced in stars trough a very complicate network of reactions and it can be easily destroyed by both proton- and α-captures [1]. Since all stars experience phases of H-burning and He-burnig during their evolutions the sites that could host the nucleosynthesis of fluorine are many. In particular, four sites have been proposed.

1. Asymptotic Giant Branch (hereafter AGB) stars are suggested to produce fluorine by means of two different processes. At solar metallicity the main chain of F production starts with ^{14}N and includes α, neutron and proton captures. While, at lower metallicities, the fluorine production is suggested to be dependent on ^{13}C ([2] and references therein).
2. Type II supernovae (SNe II) are suggested to produce cosmic fluorine via the neutrino process. Indeed the enormous quantity of neutrinos released during the core collapse could convert a significant amount of ^{20}Ne into fluorine [3].
3. Wolf-Rayet (W-R) stars, which produce F via a nucleosynthesis network similar to the one burned by AGB stars, might enrich in fluorine the interstellar medium thanks to their strong stellar winds [4, 5].
4. Hydrogen-deficient stars formed by white-dwarf merging were shown to have high carbon and fluorine abundances by [6]. However, the number of stars of this type is so small compared to the AGB stars, SNe II, and W-R stars, that their contribution to the galactic fluorine abundance is negligible.

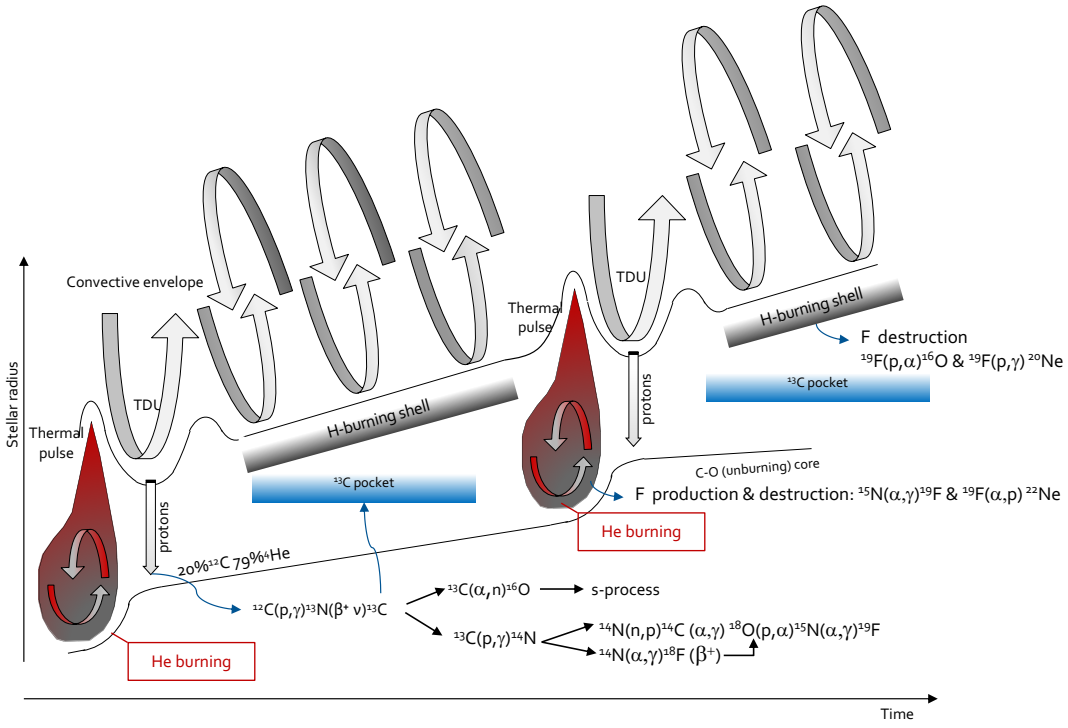

Figure 1. Cartoon showing the temporal evolution of the internal structure of an AGB star. The "drop" structures are thermal pulses (see text for details) and the sites of fluorine production and destruction are indicated by arrows linked to the nucleosynthesis reactions that take place in the different regions of the star. The labels indicate the places of the H-burning shell, the He-shell, the ^{13}C-pocket and the convective envelope.

AGB stars are commonly considered sites for the production of fluorine, because of the enhanced abundance of the element observed in a large sample of stars showing the characteristic line at $\lambda = 2.3358$ μm in their spectra (see e.g. [7] and references therein). However the the question is not whether AGB stars synthesize fluorine, but whether their production is sufficient to account for its cosmic abundance. A way to determine the site of fluorine production and to disentangle among the nucleosynthesis mechanisms suggested is to compare the observed fluorine abundance with those of other elements, whose stellar origins are well known, e.g, oxygen that is produced mainly in SNe II. This was done by [8], which observed [F/Fe] versus [Fe/H] and [F/O] versus [O/H] trends in a sample of 49 nearby, bright K giants. Both the trends were found to increase and this fact hints that ν-process could not be the dominant fluorine producer in the solar neighborhood. This findings foreseen the hypothesis that AGB stars are the main site of fluorine production in galaxies even if other authors, using different models of galactic chemical evolution, state that the yields from AGB stars are not enough to account for the whole fluorine abundance in the Milky Way [7].

In principle the resulting abundance of a nucleus (or an element) can be larger than theoretical predictions because the production channels are more efficient than thought or because destruction mechanisms are less. In this paper we investigate this latter hypothesis by employing in a code for AGB nucleosynthesis calculations the ^{19}F(α,p)^{22}Ne and ^{19}F(p,α)^{16}O reaction rate recently measured at astrophysical energies by the Trojan Horse Method (hereafter THM).

2. Fluorine Nucleosynthesis in AGB stars

The AGB phase represents an evolved stage of stars with mass smaller than 6-8$M_{\odot}$. During this phase the stellar core (made of C and O) is degenerate and the main source of energy is the thin radiative H-burning shell placed below the extended and cold convective envelope. Between the H-shell and the CO core there is a region rich in He (the He-shell), where episodes of convective He-burning periodically occur, these instabilities are known as *thermal pulses* (TP). At the end of each pulse the convective envelope penetrates into the inner stellar region bringing into the surface the fresh product of the stellar nucleosynthesis, this phenomenon is known as *third dredge-up* (hereafter, TDU).

AGB stars have been extensively studied in the last 30 years because they are important sites for the production of nuclei heavier than Fe via the s-processing (or slow neutron captures). It takes place in the He-shell during the TPs, thanks to neutrons delivered by the ^{22}Ne(α,n)^{25}Mg reaction, as well as during the H-burning phase in the He-rich intershell region where neutrons are released by the ^{13}C(α,n)^{16}O reaction. The formation of a ^{13}C reservoir just below the H-shell has been investigated by several authors because of its crucial role for the s-process. In this paper we will not enter in details of the so called ^{13}C-pocket formation, but it is important to remind that this is due to an injection of protons in the stellar layers rich in ^{4}He and ^{12}C during the TDU, which triggers the reaction chain: ^{12}C(p,γ)^{13}N(β)^{13}C. Whenever the amount of injected protons is sufficiently large, also ^{14}N is produced by further proton captures on ^{13}C. Since ^{14}N has a very large neutron capture cross section, its production has to be avoided to guarantee an efficient production of heavy nuclei via the s-process. However, the ^{14}N is the seed of the ^{19}F production, which follows the path ^{14}N$(\alpha,\gamma)^{18}$F$(\beta^{+}\nu)^{18}$O(p,α)^{15}N$(\alpha,\gamma)^{19}$F or, alternatively, the chain ^{18}O(p,α)^{15}N$(\alpha,\gamma)^{19}$F, if protons are released by the ^{14}N(n, p)^{14}C reaction [9, 10]. When the He-rich materials are engulfed in a TP (at T $\geq 2.5{\cdot}10^{8}K$) part of the ^{19}F is consumed by the ^{19}F(α,p)^{22}Ne , which is the main channel for its consumption in low-mass AGB stars. In this contest if some unburned ^{13}C is still available a further contribution to ^{19}F might still be possible via the ^{15}N$(\alpha,\gamma)^{19}$F reaction, but this rare possibility will not be considered in this work.

A further destruction of the F can also be operated by the H-burning shell, where the temperatures are not high enough to produce ^{19}F via proton capture on ^{16}O, but are in any case sufficient for its burning by the ^{19}F(p,α)^{16}O and the ^{19}F(p,γ)^{20}Ne reaction (being the first the most efficient one). Furthermore, proton captures at a few $10^{7}K$ coupled with non convective exchanging of matter between the border of the convective envelope and the H-burning shell (called extra-mixing [21]) can reduce the surface abundance of fluorine in AGBs of less than 3 $M_{\odot}$ [11].

A scheme of the complicate network of reactions responsible for fluorine nucleosynthesis is shown in Figure 1 as long with the temporal evolution of the internal structure of an AGB star.

3. Investigation of the ^{19}F(p,α)^{16}O and ^{19}F(α,p)^{22}Ne reaction via the Trojan Horse Method

Despite its importance, before 2011 [12], no data were available for the ^{19}F(p,α)^{16}O at astrophysical energies (E$_{\rm c.m.}$ $\leq$ 300 keV, where fluorine burning is most effective and widely adopted compilations such as the NACRE [13] used data from different sources to supply a recommended astrophysical factor and reaction rate. Firstly [12] observed three resonances in the energy regions of interest for the study of stellar nucleosynthesis by using the indirect experimental technique called Trojan Horse Method. According with [14], and references therein, through this technique a two body reaction (having two massive particle in the exit channel) can be measured down to the Gamow-peak energy region by performing a three-body reaction at a beam energy that allows to overcome the Coulomb barrier in the reaction entrance channel as well as the electron screening. Via the THM the cross-section of the two-body ^{19}F(p,α)^{16}O has been determined by properly selecting the quasi-free contribution of the three-body reaction ^{2}H(^{19}F, α^{16}O)n, where n plays the role of the spectator particle and ^{2}H acts as the TH nucleus because of its p$\oplus$n cluster structure.

Three THM experiments were performed [12, 11, 15] that have shown the presence of resonant structures at E$_{\rm cm}$ $\leq$ 0.6MeV and hinted to an enhancement of he reaction rate at astrophysical temperatures (about $10^{7} - 10^{8}K$). In particular around the E$_{\rm cm}$ 0.794 MeV resonance, all the data agree reasonably well, while in the E$_{\rm cm}$0.6MeV energy range, the S(E) factors extracted from the most recent experiment [15] is larger because of a resonance at 251 keV, which had not been observed before by [12, 11], but whose presence was also confirmed by

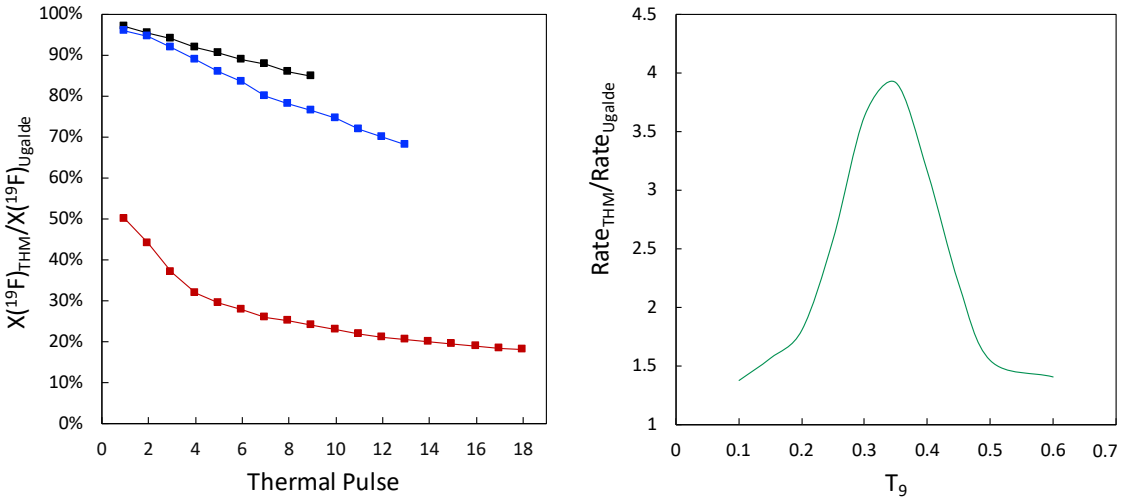

Figure 2. Left panel. Temporal evolution of the ratio between the ^{19}F abundance in the He-shell obtained by adopting the ^{19}F(α,p)^{22}Ne reaction rate determined via THM and the one calculated by [17]. Each dot refers to a thermal pulse (see text for details). The black, the blue and the red curve refer to AGB models of 1.5, 3, and 5 $M_{\odot}$, respectively. Right panel. Ratio between the THM recommended value of the ^{19}F(α,p)^{22}Ne rate and the value recommended by [17], as a function of the temperature in units of GK.

the data extracted from [16]. From R-matrix calculation it turns out that the difference among the THM reaction rate at T_9=0.04-0.2 are small ($\sim$ 10%) while larger discrepancy ($\sim$ 30%) is found at a temperature $T_9 \geq$0.04. For a comparison of the reaction rates and details on data analysis we refer to figures 13-16 in [15].

The THM has been successfully applied also to investigate the ^{19}F(α,p)^{22}Ne, which is hard to be directly studied because the Coulomb barrier is at about 3.1MeV and the energy range typical of stellar He-burning is 200-1100keV. In this framework the lowest energy at which the reaction has been directly measured is 660 keV [17] and data available in literature were affected by large uncertainties. The reaction chosen to investigate the ^{19}F(α,p)^{22}Ne via the THM was the ^{19}F(^{6}Li, p^{22}Ne)^{2}H because of the well-known cluster structure of the ^{6}Li nucleus ($\alpha \oplus d$), which under proper kinematical conditions allows us to consider the deuteron particle as a spectator. The common findings of [18] and [19] is an increase of the ^{19}F(α,p)^{22}Ne reaction rate up to a factor of 4 respect to the direct data available in literature [17] in the energy region of stellar nucleosynthesis. Such an enhancement can be seen in Table 4 of [19] and in the right panel of figure 2.

4. THM Reaction Rate Implications in AGB star nucleosynthesis

Our study of the implications of the THM reaction rates of the ^{19}F(p,α)^{16}O and ^{19}F(α,p)^{22}Ne to fluorine nucleosynthesis in AGB stars was performed in two steps. Firstly the fluorine production/destruction in the He-rich stellar layers (during both the H-burning periods and the TPs) was investigated in the light of the ^{19}F(α,p)^{22}Ne rate estimated by the THM [18, 19]. In particular, calculations for three stellar models of 1.5, 3, and 5 $M_{\odot}$ and solar metallicity were performed by the NEWTON code [20]. To better appreciate the effects of the α-capture reaction rate, phenomena of ^{19}F destruction due to proton captures, such as the extra-mixxing ([21] and references therein) or hot bottom burning (in the case of the 5$M_{\odot}$ model, [22]) were not considered in the first step of our analysis. As explained before, the mechanism for formation of the ^{13}C-pocket might have important implication also for the fluorine nucleosynthesis, in this paper we adopt the profile for proton injection in the inter-shell and the resulting pockets of ^{13}C and ^{14}N suggested by [23] and [24], the same cross-sections for neutron capture reactions used by the quoted authors, and the reaction rates of proton and alpha captures reported in Table 5 by [19].

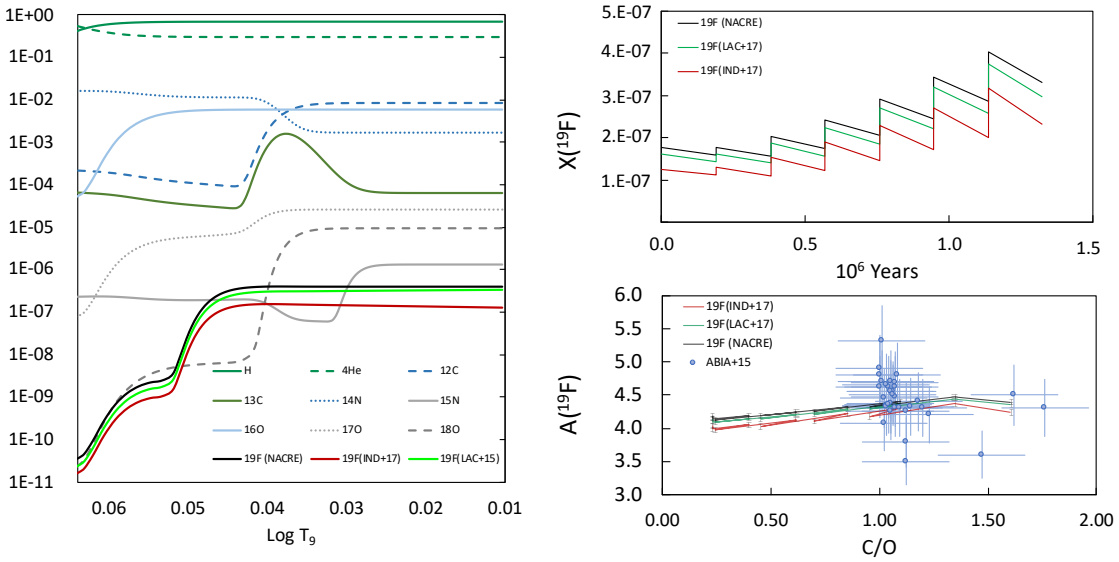

Figure 3. Left panel. Isotopic composition of the H-shell of our $2M_{\odot}$ and solar metallicity AGB model. Abundances of F and of the nuclei participating into the CNO cycle are shown as a function of the logarithm of the temperature measured in GK. The stellar radius proceeds from the right to the left. Three curves deal with the fluorine abundance profile computed by using the ^{19}F(p,α)^{16}O reaction rate by [13] (black line), [11] (green line) and [15] (red line). Upper right panel. Temporal evolution of the surface abundance of ^{19}F in the $2M_{\odot}$ and solar metallicity AGB model. The stepwise trend is due to the enrichment in F at each TDU (which brings into the envelope the ashes of the He-burning) and the F destruction of the extra-mixing during the H-burning periods. The three curves show the model outputs obtained with the three ^{19}F(p,α)^{16}O reaction rate we are studying. Lower right panel. Comparison between the same model output reported in the upper panel and the abundances observed in a sample of AGBs by [7]. The F abundance are given using the definition A(^{19}F) = 12 + log(X(^{19}F)/H), being (X^{19}F/H) the abundance of ^{19}F by number, and are reported as a function of the C/O ratio.

The left panel of Figure 2 shows the temporal evolution during the whole AGB phase of the ratio between the ^{19}F abundance obtained in the He-rich stellar region after each TP by adopting the ^{19}F(α,p)^{22}Ne reaction rate determined via THM and the one calculated by using the rate published in [17]. The black, the blue and the red curve refer to AGB models of 1.5, 3, and 5 $M_{\odot}$, respectively. As illustrated by the right panel of figure 2, at the typical temperature of the He-shell burning, the THM rate is always larger than the one by [17]. As a consequence, ^{19}F is more easily destroyed during TP and the abundances predicted in the stellar interior are smaller. The 5 $M_{\odot}$ AGB model shows the largest sensitivity to the reaction rate used in calculations, indeed in its He-shell the ^{19}F abundance is reduced down to a factor of 4 in the last pulses. This is so because the He-burning temperature reaches $3.6{\cdot}10^{8}K$ that corresponds to the energy at which the difference between the THM cross-section and the [17] one is maximum. Smaller variations are registered in the 1.5 and 3 $M_{\odot}$ models, where temperatures in the He-shell are lower. However, once the ashes of the He-burning are brought into stellar surface by TDU, the nucleosynthesis products are diluted with envelope materials and the effects of the ^{19}F(α,p)^{22}Ne reaction rate become negligible. None of the studied cases shows a variation in the ratio larger than 5%. An extended discussion on the implication to the F production/destruction in AGB stars of the ^{19}F(α,p)^{22}Ne rate measured by the THM can be found in [19], these authors also present the effects of using the upper limit and the lower limit of the rate in nucleosynthesis calculations.

In the second phase of our analysis the destruction of fluorine due to burning of the ^{19}F(p,α)^{16}O reaction in the H-shell was studied. In doing so the composition of the H-burning

shell of $2M_{\odot}$ and solar metallicity AGB stars was computed by the SHELL nucleosynthesis code [21, 25]. The left panel of figure 3 shows the three profile of the ^{19}F abundance computed by using the ^{19}F+p rata published by [11], [15] and [13], being the first two measured by the THM. As expected the fluorine abundances are lower in models that employ a larger reaction rate. Moreover, the post-process code MAGIC [21, 25] was run to estimate the dilution of the surface F abundance due to extra-mixing[1] in the light of the three rates of the ^{19}F(p,α)^{16}O reaction ([11], [15] and [13]). Results are reported in the upper panel on the right of Figure 3, where the profiles of the fluorine abundance in the envelope of a $2M_{\odot}$ and solar metallicity AGB are drawn as a function of the time, from the beginning of the AGB phase. Finally, in the lower panel on the right of Figure 3, the predictions of our models are compared with the F abundance observed in a sample of AGB stars [7]. Despite the choice made for the ^{19}F(p,α)^{16} cross section, the three models are all in a quite good agreement with the observations. All reported results refer to calculations and comparisons made using only the recommended values of the ^{19}F(p,α)^{16}O reaction rate. By considering the uncertainties of the 3 estimates of the reaction rate we find that the nucleosynthesis predictions agree the one with the others within the error bands. In any case it is evident (in particular from the lower panel on the right of figure 3) that the major uncertainties are those coming from the stellar observations.

5. References

[1] Lugaro M., Ugalde C., Karakas A. I., et al. 2004 *ApJ* **615** 934
[2] Cristallo S., Di Leva A., Imbriani G., et al. 2014 *A&A* **570** 46
[3] Woosley S. E., & Haxton W. C. 1988 *Nature* **334** 45
[4] Meynet G. & Arnould M. 2000 *A&A* **355** 176
[5] Palacios A., Arnould M., & Meynet, G. 2005 *A&A* **443** 243
[6] Longland R., Lorén-Aguilar P., José J., et al. 2011*ApJL* **737** 34
[7] Abia C., Cunha K., Cristallo S., et al. 2015 *A&A* **581** 88
[8] Jönsson H., Ryde N., Spitoni E., et al. 2017 *ApJ* **835** 50
[9] Cristallo S., Straniero O., Gallino R., et al. 2009 *ApJ* **696** 797
[10] Forestini M., Goriely S., Jorissen A., & Arnould, M. 1992 *A&A* **261** 157
[11] La Cognata M., Palmerini S., Spitaleri C., et al. 2015 *ApJ* **805** 128
[12] La Cognata, M., Mukhamedzhanov, A. M., Spitaleri, C., et al. 2011 *ApJL* **739** 54
[13] Angulo C., Arnould M., Rayet M., et al. 1999 *NuPhA* **656** 3
[14] Spitaleri C., La Cognata M., Lamia L., et al. 2016 *EPJA* **52** 77
[15] Indelicato I., La Cognata M., Spitaler C., et al. 2017 *ApJ* **845** 19
[16] Lombardo I., Dell'Aquila D., Di Leva A., et al. 2015 *PhLB***748** 178
[17] Ugalde C., Azuma R. E., Couture A., et al. 2008 *PhRvC* **77** 035801
[18] Pizzone R. G., D'Agata G., La Cognata M., et al. 2017 *ApJ* **836** 57
[19] D'Agata G., Pizzone R.G., La Cognata M, et al. 1992 *ApJ* **860** 61
[20] Trippella O., Busso M., Maiorca E., et al. 2014 *ApJ* **787** 41
[21] Palmerini S., La Cognata M., Cristallo S., & Busso M. 2011 *ApJ* **729** 3
[22] Sackmann I. J., & Boothroyd A. I. 1992 *ApJ* **392** L71
[23] Trippella O., Busso M., Palmerini s., et al. 2016 *ApJ* **818** 125
[24] Palmerini S., Trippella O., Busso M., et al. 2018 *Ge.Co.A.* **221** 21
[25] Palmerini S., Cristallo S., Busso M., et al. 2011 *ApJ* **741** 26
[26] Palmerini S., Trippella O., Busso M. 2017 *MNRAS* **467** 1193

[1] The extra-mixing model we use is the one described in [26]